

1 **Modeling of coastal erosion in exposed and groin-protected steep** 2 **beaches.**

3 Juan L. Garzon¹, Oscar Ferreira², and Theocharis A. Plomaritis³

4 ¹ Postdoctoral Research, CIMA – Centre for Marine and Environmental Research, FCT, Universidade do Algarve, Campus de Gambelas,
5 8005-139 Faro, Portugal. jlhervas@ualg.pt

6 ² Associate Professor, CIMA – Centre for Marine and Environmental Research, FCT, Universidade do Algarve, Campus de Gambelas,
7 8005-139 Faro, Portugal. oferreir@ualg.pt

8 ³ Lecturer, Faculty of Marine and Environmental Science, Department of Applied Physics, University of Cadiz, Campus Rio San Pedro
9 (CASEM), Puerto Real 11510, Cadiz, Spain. haris.plomaritis@uca.es

10 **ABSTRACT**

11 Process-based models are suitable tools for reproducing storm-driven erosion. However, their performance has been mainly
12 examined on mild-slope sandy beaches and their use on steep beaches represents still a challenge. Here, XBeach experiments were
13 combined with topographical measurements collected for two storms (16-yr and 5-yr return period) to obtain a reliable model. The model
14 parameters “facua” (parameterized wave asymmetry and skewness sediment transport component), “bermslope” (upslope transport term
15 for semi-reflective beaches), and “wetslope” (critical avalanching submerged slope) were utilized for calibration and validation. The 16-yr
16 storm simulations on an exposed beach revealed that whether “bermslope” increased, “facua” must be reduced, and vice versa, to properly
17 simulate erosion. Adding “bermslope” provided excellent results for these storms when using “facua” and “wetslope” values close to the
18 recommended values. In a groin-protected site, XBeach was successfully calibrated and validated for the tested storms using these
19 parameters, although with different values. These experiments demonstrated that the appropriate use of these parameters can satisfactorily
20 simulate morphological changes on steep beaches for different hydrodynamic conditions and coastal settings (exposed and groin-
21 protected).

22 **INTRODUCTION**

23 Sandy coasts are among the most populated areas worldwide and they host a large number of socio-economic activities.
24 However, these environments are susceptible to the impact of coastal storms, with storm surges and waves generated during energetic
25 events causing severe erosion and shoreline retreat. Moreover, this problem might be exacerbated by rising sea levels and changes in
26 storminess. Under these threats, predicting erosion due to extreme oceanic events is essential to improve coastal management and

27 implement mitigation measures (e.g. early warning systems) that contribute to avoiding or minimizing their effects in socioeconomic
28 activities and ecosystems services. Among the different alternatives to support engineers and decision-makers, morphodynamic numerical
29 models are increasing their popularity. For instance, the open-source process-based model XBeach (Roelvink et al. 2009) has been applied
30 and validated in many sandy beaches worldwide impacted by severe tropical and extratropical storms. This model solves wave breaking,
31 surf and swash zone processes, dune erosion, and overwashing in a one-dimensional or a horizontally two-dimensional computational grid
32 under the assumption of a saturated surf zone, mainly occurring in dissipative beaches.

33 Dissipative beaches present a mild slope in the intertidal region and wave processes are dominated by skewed and asymmetric
34 short-crested waves, undertow, and infragravity waves. Several modeling studies have focused on these types of environments (e.g.
35 McCall et al. 2010; van der Lugt et al. 2019) demonstrating that, after a calibration process, XBeach can properly simulate coastal
36 morphological changes of the subaerial beach during storm events. On the other hand, the storm-induced morphological response in less
37 dissipative beaches has not been widely numerically investigated yet. Steep sandy beaches can be found in many regions including
38 Portugal, New Zealand, the south-eastern coast of Australia, the Californian coast, etc., yet, the modeling of coastal erosion in intermediate
39 and reflective sandy beaches is still an ongoing challenge (Roelvink and Costas 2017). In reflective beaches, the energy of the incident
40 waves and the subharmonic oscillations may dominate in the inner surf and swash zone against the undertow and the infragravity waves.
41 Thus, the modeling of the subaerial profile morphology without considering the evolution and decay of individual waves becomes
42 complicated at these beaches. Orzech et al. (2011) stated that the XBeach (surfbeat) underestimates the uprush sediment transport in the
43 swash zone at steep beaches, relative to the offshore transport induced by the backwash, leading to excessive removal of sediment in the
44 beach face. Consequently, special caution is required for the model parametrization when developing prediction systems in non-dissipative
45 beaches.

46 In preceding studies (Simmons et al. 2019; Vousdoukas et al. 2012b), erosion overestimation was partially overcome by
47 increasing the parameterized wave asymmetry and skewness sediment transport component (“facua”). This enhances the onshore sediment
48 transport that counteracts the offshore one induced by the wave rundown, promoting a better calibration for beach erosion. In line with this
49 approach, Elsayed and Oumeraci (2017) found a power function relation between the average slope steepness and “facua”. Nevertheless,
50 Simmons et al. (2019) stated that increasing “facua” improves the prediction in the dune and berm but unrealistically flattens the modeled
51 beach profile around the waterline. They noticed that in steep profiles the measured post-storm profile retreated but maintained a similar
52 pre-storm slope. To reproduce this observed behavior, Roelvink and Costas (2017) proposed a pragmatic approach where the beach face
53 slope is forced to stay close to a given slope, “bermslope”. Therefore, an onshore transport term that is proportional to the difference
54 between the actual slope and a prescribed “bermslope” is added in the swash zone. While this transport term was initially thought for

55 improving the reliability of the XBeach model in the long-term simulations, Roelvink et al. (2019) demonstrated that this new addition has
56 a beneficial effect on the profile evolution during storm events on steep beaches. Moreover, they suggested that “bermslope” could
57 minimize the importance of other slope parameters implemented in the model such as “wetslope”, which establishes the critical bed-slope
58 of the wet profile before the initiation of avalanching. Cho et al. (2019) declared that XBeach is more sensitive to changes in “wetslope”
59 values in a steep profile than in a mild profile, and hence, the selection of this parameter should be carefully considered in these beaches.

60 In terms of computational effort, using a 1D approach to calibrate a model instead of a 2D model would be more efficient since
61 it would allow for a more rapid assessment of all free model parameters, especially for highly complex, process-based models. The
62 downside of this approach is that the findings of a 1D calibration model might not be directly applied to a detailed 2D model. Cross-shore
63 profile models have the inherent limitation of longshore uniformity, and they are not capable of capturing the effects of longshore transport
64 gradients. Conversely, the 2D models incorporate longshore variations, and they are not limited to straight-line coastal systems, being able
65 to represent diverse coastal geometries (e.g. Dissanayake et al. 2014; McCall et al. 2010; Plomaritis, 2018; van der Lugt et al. 2019). A
66 few studies (Dissanayake et al. 2014; Harter and Figlus 2017) have conducted a more efficient approach, optimizing a 1D XBeach model
67 and then transferring the optimum settings to a larger 2D XBeach model. This practice might avoid excessive computational burdens when
68 designing an EWS; yet, the downside of such an approach was not fully investigated.

69 While process-based models seek to explicitly represent the crucial physical dynamics, in practice, they include semi-empirical
70 parameterizations to improve their efficiency. This results in a large number of free model parameters to calibrate, especially for coastal
71 morphologies where research efforts have been less intense (e.g. steep beaches). The constant evolution of the models implies the
72 necessity of continuous calibration and validation. Also, calibration parameters vary according to the specific characteristics of each site.
73 The present study has a twofold objective: firstly, to perform a sensitivity analysis of the main morphological parameters used for XBeach
74 calibration (“facua”, “bermslope”, and “wetslope”); and secondly, to use the above results to calibrate and validate XBeach for two storm
75 events with different severity at two steep beaches with different levels of human intervention. The results will contribute to obtaining
76 better model performances in such environments. Moreover, in cases where the available data for model calibration and validation are
77 limited, recommendations for the model implementation are indicated.

78 **STUDY AREA**

79 **Praia de Faro**

80 Praia de Faro is a sandy beach located in the barrier island system of Ria Formosa, on the southern Portuguese coast (Fig. 11 –
81 III). The barrier splits the Atlantic Ocean on the front side from a coastal lagoon on the backside (Fig. 1 IV). The study site is an elongated

82 peninsula orientated 130° approximately (measure from the north). This beach is subject to significant urban development pressure and the
83 oceanfront is partially stabilized with rocks/walls or naturally protected by a dune. The dune morphology varies alongshore with higher
84 robustness and elevation (7-8 m above mean sea level, MSL) at the western portion of the study area (F6 in Fig. 1 IV), while at the central
85 and eastern part, the dune is lower (6-7 m above MSL) and weaker. The central part, F4 and F5 in Fig. 1 IV, is periodically overtopped
86 during spring tides or storm conditions (Ferreira et al. 2019; Matias et al. 2010). The site presents a sub-tidal terrace, steep beach face, with
87 an average slope of around 0.10 (Vousdoukas et al. 2012a). In previous studies such as Ferreira et al. (2016), this site has been classified as
88 reflective during calm conditions and intermediate during energetic conditions with the formation of a longshore bar. A beach berm can be
89 normally found, except after very energetic storms, with variable widths ranging from less than 15 m to more than 40 m (Ferreira et al.
90 2016). The study area responds rapidly to storm events and variations of the wave forces, and the beach can regain a large part of the
91 sediment after storm events in days/weeks. Moreover, the site is characterized by the presence of multiple highly dynamic beach cusps at
92 the lower beach face that interact with the more persistent upper beach face cusps (Vousdoukas et al. 2012a). Sediments are medium to
93 very coarse, moderately well-sorted sands with median (d_{50}) around 500 μm and d_{90} around 2000 μm (Vousdoukas et al. 2012b).

94 **Quarteira**

95 The town of Quarteira is located ten kilometers from Praia de Faro towards the northwestern direction (Fig. 1 III). The analyzed
96 sector consists of a set of three sandy beaches with a total longshore length of 900 m. The main orientation of the coastline is 120°N and
97 the average beach slope is 0.10. Sediment grain size is slightly finer than in Praia de Faro and d_{50} and d_{90} are 485 μm and 900 μm
98 respectively. The three beaches are laterally limited by 150 m length rocky groins (Fig. 1 V). These groins make the three beaches behave
99 like “manmade pocket beaches” subject to beach rotation as a function of wave direction. During the dominant conditions, the groins
100 maintain the sediment in the system; however, during very energetic conditions the sediment can fall outside of the system. Beach
101 nourishments have been performed at the area to guarantee a reasonable beach width for bathing conditions, with a total of 360000 m^3
102 placed in 1998 (Pinto et al. 2018). At the backside, the beach is limited by a long promenade with an elevation ranging from 6 to 8 m.
103 While Quarteira represents a relevant touristic destination in Portugal, the beach morphodynamic has been poorly investigated.

104 **METHODS**

105 **Storm events**

106 Two storms impacting the area have been considered for analysis. Storm Emma, in March 2018, was a severe storm that traveled
107 towards the northeastern direction (Ferreira et al. 2019). The maximum significant wave height, H_s , measured at the Faro buoy during this
108 storm was 6.55 m, with a peak period and direction of 13 s and 240°N respectively (Fig. 2). Moreover, the timing of the storm matched

109 with a spring tide, exacerbating the impact of the storm. Large damages were reported after the storm, especially in Praia de Faro (Ferreira
110 et al. 2019). In December 2019, two consecutive storms hit the area, storm Daniel (December, 16) and storm Elsa (December, 19-20).
111 These storms traveled across the North Atlantic from east to west and their effects were widely felt in several western European countries.
112 Storm Elsa created H_s up to 5.15 m and 11 s peak period, at the Faro buoy (Fig. 2). This storm coincided with neap tides, probably
113 reducing the negative erosive effects of the storm. Maximum H_s and peak period during Daniel were 3.85 m and 9 s, respectively.

114 Based on the analysis of Pires (1998), storm Emma corresponds to a 16-yr storm (Ferreira et al. 2019), Elsa is a 5-yr storm and
115 Daniel is a 1-yr storm. Moreover, at Praia de Faro, during storm Emma, the collision regime was observed in sections where the dune
116 system is higher, while in sections where the dune is less strong and lower overwash occurred. Storm Elsa caused mainly swash regime
117 and collision regime was only observed in sections with a limited berm, and only swash regime occurred during storm Daniel. Therefore,
118 for the southern Portuguese coast, storms Emma, Elsa and Daniel can be defined as high-energy, mid-energy, and low-energy events
119 respectively.

120 **Morphological dataset**

121 To assess the ability of XBeach to model morphological changes during those storms, several topographic datasets were
122 collected (Table 1). At Praia de Faro, after the peak of storm Emma, on March 2, 2018, five profiles, F2-F6 (Fig. 1 IV), were surveyed
123 with a DGPS (Differential Global Positioning System). Within the COSMO program (PROGRAMA COSMO n.d.), an unmanned aerial
124 vehicle (UAV) survey and a bathymetric survey were conducted at Praia de Faro in October 2018. The surveys covered the entire study
125 site, including the nearshore area (13.5 m below MSL), beach face, dune system, and the urbanized area. The mean vertical error of the
126 October 2018 survey along five profiles ranged between 0.14 and 0.20 m, considering the DGPS survey as the benchmark. Finally, another
127 survey was conducted on December 20, 2019, to measure the elevation of 4 profiles, F1, F2, F3, and F5, after storm Elsa.

128 On the Quarteira site, three surveys were conducted. Firstly, on May 28, 2019, a Mavic 2 Pro UAV, was used to obtain a digital
129 elevation model (DEM) and Orthophoto map of the study area (Table 1). A total of 45 ground control points (GCP) were marked at the
130 fixed structures and at the beach to build the DEM. The elevation of the DEM was compared against 4 cross-shore profiles measured and
131 the estimated Root Mean Square Error (RMSE) of the entire area was 0.09 m. The built DEM presented a resolution of 0.014 m, while the
132 Orthophoto had less than 1 cm of resolution. Secondly, two consecutive surveys were performed by using DGPS along nine profiles (see
133 Fig. 1 V), on December 17, 2019, before storm Elsa and December 20, 2019, after storm Elsa.

134 Two complementary sources were utilized to extract the elevation of the sea bottom in offshore areas of the model domains. The
135 Agência Portuguesa do Ambiente (APA) surveyed the nearshore areas of the Quarteira site in 2018. The processed information covers

136 from -1 m to -8 m MSL. Moreover, a regional bathymetry of the entire Southern Portuguese continental shelf was extracted from
137 MIRONNE (Luis 2007) to cover the deepest region of the grid models. Both datasets have a resolution of 10 m.

138 The comparison of the different profiles measured along Praia de Faro (Fig. 1 IV) together with those reported in Ferreira et al.
139 (2019) and Garzon et al. (2020) allowed defining a fully developed berm and a weak-berm profile, which are representative of this site.
140 The first one with a beach face slope of 0.13, had a well-developed berm around the 4.4 m elevation and the dune toe was found at 5 m
141 (Fig. 3 a). The second profile displayed a beach face slope of 0.12 and the dune toe was located at 4.6 m. The berm of this profile was less
142 marked than the previous profile being therefore named weak-berm (Fig. 3 b). The vertical datum of the aforementioned elevation data
143 was MSL as well.

144 **XBeach model setup**

145 The Praia de Faro 2D grid had an extension of 3000 m longshore and 3900 m cross-shore (
146 Fig. 1 III). The numerical grid, with a variable longshore and cross-shore grid cell spacing, was built using the OpenEarth tool (Van
147 Koningsveld et al. 2010). The grid optimization and interpolation were made based on the bathymetry data from the COSMO program
148 survey (PROGRAMA COSMO, n.d.) and the continental shelf referred to MSL. The minimum cross-shore and alongshore resolution in
149 the sub-aerial beach were 2 m and 10 m, respectively. Using satellite imagery available via Google Earth, parking lots, infrastructures and
150 building locations were identified and superimposed to the grid. At those locations, grid cells were set as a non-erodible layer. Therefore,
151 these grid cells cannot be eroded or destroyed. This has important implications on Praia de Faro where the seawall impedes erosion to
152 reach the urbanized areas during severe storms (Ferreira et al. 2019). The 1D simulations were performed in cross-shore profiles extracted
153 from the 2D grid at specific locations (F2, F3, F4, F5, F6), and thus, they maintained the same cross-shore resolution of the 2D grid model.

154 In Quarteira, two 2D grids were built using the OpenEarth tool. These grids shared geometry, domain, and resolution but
155 differed in the intertidal and the dry region elevation to account for two different initial topographies. Regarding the topography, two
156 datasets were used: a) the two-dimensional unmanned aerial survey of May 28, 2019, (hereafter the Quarteira May grid), and b)
157 interpolation of the nine profiles measured on December 17, 2019, (hereafter the Quarteira December grid), into a two-dimensional
158 elevation model of the dry beach combined with the elevation of the groins measured in the May 2019 survey. The dimension of the grids
159 was 1100 m longshore by 5800 m cross-shore (Fig. 1 III). The grids presented a variable resolution with a minimum resolution of 2 m and
160 5 m in the cross-shore and longshore directions. The longshore resolution was reduced to better capture the groin geometry. The nearshore
161 bathymetry measured by APA and the regional bathymetry of the continental shelf were merged to cover offshore and nearshore areas.

162 Rocky groins and infrastructures determined as non-erodible in the model were identified from the orthophoto. The grid model elevation
163 was referred to MSL.

164 This study used the XBeachX 1.23.5526 version with lateral Neumann conditions in the non-linear shallow water equations and
165 cyclic wave boundary conditions. The “single_dir” option was selected to simulate the propagation of the directionally-spread short waves
166 group in the 1D and 2D models. In the 2D approach, the mean wave direction was intermittently computed using the stationary solver
167 within XBeach and then, it propagated the wave energy along these directions. Thus, it preserved the groupness of the wave, leading to
168 higher forcing on the infragravity waves (Roelvink et al. 2018). In the 1D, “single_dir” used a single directional bin, considering waves
169 reaching normally to the coast and ignoring refraction (Documentation XBeach 2018). To support transferability, many of the XBeach free
170 parameters that can impact the ability of the model to predict morphological changes were either maintained their default value or
171 substituted by values reported in the literature (Table 2). For instance, in the absence of wave measurements in the surf zone, the breaker
172 parameter, “gamma” was set to 0.56 as suggested by Callaghan et al. (2013). The parameters “gamma” (maximum ratio wave height to
173 water depth) and “beta” (the breaker slope of the roller) were set to 2.364 and 0.138 following the values reported by Do et al. (2018), a
174 study that investigated the modeling of dune erosion. In order to reduce the number of parameters to calibrate, the Manning’s coefficient
175 associated with bed roughness was based on land-cover classification for sandy sediment (Garzon and Ferreira 2016; van der Lugt et al.
176 2019). Also, a morphological acceleration factor of 10 was applied following previous studies such as McCall et al. (2010).

177 A SWAN model (Booij et al. 1999) was created for the Southern Portuguese coast to propagate the wave conditions from the
178 Fig. 1 II). The grid was curvilinear to match the variations of the bathymetry with a varying resolution (from a few km to hundreds m).
179 SWAN outputs from the nonstationary computations were extracted at the offshore boundary of the XBeach computational grids, between
180 25 and 30 m water depths (Fig. 1 III). The wave conditions considered in the XBeach simulations for each storm are displayed in Fig. 2. In
181 the SWAN computations, water levels did not experience variations and model parameters were maintained by default.

182 **Assessed XBeach parameters**

183 As previously expressed, three model parameters (“*facua*”, “*bermslope*”, and “*wetslope*”) that may have a strong influence on
184 the morphodynamics were investigated. The parameter “*facua*” is very relevant in the morphological module as it mainly governs the net
185 cross-shore sediment transport (Elsayed and Oumeraci 2017). As XBeach only simulates short wave energy averaged over a wavelength
186 (wave phase is not considered), the sediment advection velocity u_a responsible for stirring the sediment and transporting it to the shore
187 must be approximated. Van Thiel de Vries (2009) proposed an expression to indirectly calculate that velocity as a function of a wave
188 skewness parameter (S_k), a wave asymmetry parameter (A_s), the root mean square velocity (u_{rms}) and “*facua*” following the form:

$$189 \quad u_a = \textit{facua} u_{rms} (S_k - A_s), \quad (1)$$

190 In shallow areas, with highly nonlinear waves, higher values for u_a are expected since the difference between S_k and A_s increases and
191 consequently, larger onshore sediment transport due to the wave nonlinearity occurs.

192 Another parameter investigated affecting the cross-shore sediment transport was “bermslope”. Under the assumption that the
193 intertidal beach slope remains relatively stable in intermediate and reflective beaches, Roelvink and Costas (2017) proposed a simple
194 mechanism to address the challenge of simulating intertidal beach slopes in long-term simulations. Later, Roelvink et al. (2019) extended
195 the method to two dimensions. In XBeach the sediment transport (S) is computed as:

$$196 \quad S = u_{sed} h c \quad (2)$$

197 where u_{sed} is the depth-averaged sediment advection speed, h the water depth and c the depth-average concentration.

$$198 \quad S_{swash} = S - f_{swash} |S| \left(\frac{\partial z_b}{\partial x} - \left[\frac{\partial z_b}{\partial x} \right]_{eq} \right) \quad (3)$$

199 where S_{swash} is the corrected transport, f_{swash} a transport factor (15), z_b represents the bottom elevation and x the cross-shore distance, and
200 the last term is the equilibrium slope near the waterline. This corrected transport term is only applied in the swash region, defined by a
201 limit where wave height is larger than water depth (Roelvink et al. 2019).

202 During the collision regime, dune face erosion or slumping is predominantly triggered by a combination of infragravity swash
203 runup on the previously dry dune face and the critical wet slope. In the model, this process is considered by an avalanching mechanism
204 triggered when the infragravity incursions reach the dune front and it becomes wet. The transition of the wet and dry grid cells is
205 controlled by a user-specified water depth (“ h_{switch} ”). If the critical slope between two adjacent grid wet cells is exceeded, sediment is
206 exchanged between these cells in the amount needed in order to bring the slope back to the critical slope. As a result, sediment is brought
207 from the dry dune into the wet profile, where it is transported further seaward by the undertow and infragravity backwash (Roelvink et al.
208 2009).

$$209 \quad \left| \frac{\partial z_b}{\partial x} \right| > \text{critical slope}, \quad (4)$$

210 The maximum dune erosion rate can be limited (“ dz_{max} ”). In this study, “ dz_{max} ” and critical dry slope used the default values while the
211 “ h_{switch} ” used the lowest limit within the recommended values (0.01) since the coarse material of the sites enhances water infiltration and
212 soil saturation, and thus reduces soil cohesion, and ultimately dune resistance.

213 By varying the parameter values according to a set of combinations, a sensitivity analysis of the horizontal retreat and XBeach
214 calibration and validation were performed (Fig. 4). Note that the default value of “ $facua$ ” was not considered at this evaluation since
215 previous authors recommended higher values of “ $facua$ ” for steep profiles (Vousdoukas et al., 2012b). The values proposed to
216 “bermslope” were chosen based on values found in the literature (Roelvink et al. 2019) and the average beach face slope of Praia de Faro.

217 For “wetslope”, the evaluated values covered the range of ± 0.1 around the default value (Table 3). The running test sequence is illustrated
218 in Fig. 4.

219 Firstly, storm Emma was used to assess model sensitivity, in terms of horizontal retreat of two 1D profiles, a fully-developed
220 berm and a weak-berm (Fig. 3 and Fig. 4), by applying combinations of the parameters displayed in Table 3. In total, 36 simulations were
221 performed. For each run, the erosion indicator selected was the relative horizontal displacement computed at the three elevations depicted
222 in Fig. 3 (3 m, berm crest, and dune toe) as the relative displacement with respect to the displacement simulated by using the parameter
223 combination with the lowest “facua” and “wetslope” and “bermslope” off. This combination was chosen as a benchmark because it was
224 Fig. 1 IV) were selected to reproduce the morphological changes induced by storm Emma in Praia de Faro (Fig. 4). The profiles were
225 selected due to the different morphologies that they exhibited for the same exposed beach. The model was calibrated using the parameters
226 previously studied (Table 3) and the rest of the main settings are indicated in Table 2. Thirdly, storm Emma was used to validate the 2D
227 model of Praia de Faro and to compare model discrepancies between 1D and 2D approaches (Fig. 4). Moreover, further investigations are
228 presented to better understand the role of the gravity and infragravity wave modeling approach (2D “single_dir”, 1D “single_dir”, and 1D
229 “multi_dir”) in those discrepancies. Using storm Emma as a calibration event, the model was validated for storm Elsa (Fig. 4). Fourthly,
230 in the site of Quarteira, a 2D model calibration, using storm Elsa, was carried out (Figure 4); the 1D approach was not applied for this site.
231 The parameters used for calibration are displayed in Table 3 and the rest of the main settings in Table 2. After model calibration, the role
232 played by the initial or pre-storm topography was assessed by simulating storm Elsa and Emma for both Quarteira May and Quarteira
233 December topographies (Fig. 4). These two storms were included in the analysis to study the influence of storm energy on the model
234 sensitivity to the input topography. Also, the impact of storm Emma on this site was qualitatively analysed (Fig. 4).

235 **Evaluation metrics**

236 Three typical and widely applied model skills were used: bias, RMSE and BSS. The bias is the difference, in meters, in central
237 tendencies of the predicted or modeled elevation values, $Z_{modeled}$ and the measured elevation values, $Z_{measured}$, at each considered grid cell.

$$238 \text{ Bias} = \langle (Z_{modeled} - Z_{measured}) \rangle, \quad (5)$$

239 a positive bias means that the bed level is higher in the computed data set than at the measurements (erosion underprediction). The angled
240 brackets indicate the average of the readings. The Root Mean Square Error (RMSE) is the quadratic mean, in meters, of the differences
241 between predicted values and measured values. The RMSE is determined as:

$$242 \text{ RMSE} = \sqrt{\langle (Z_{modeled} - Z_{measured})^2 \rangle}, \quad (6)$$

243 The Brier Skill Score, BSS, provides an objective method for assessing the performance of morphological models. Conversely to
244 the RMSE and bias skills, BSS is dependent on the profile morphology before the storm. The classification used, from van Rijn et al.
245 (2003), considers values between 0.8-1.0 excellent, 0.6-0.8 good, 0.3 - 0.6 reasonable, 0-0.3 poor and below 0 bad. The BSS can be
246 computed as:

$$247 \text{ BSS} = 1 - \frac{\langle (Z_{\text{measured}} - Z_{\text{modeled}})^2 \rangle}{\langle (Z_{\text{measured}} - Z_{\text{initial}})^2 \rangle}, \quad (7)$$

248 where Z_{initial} represents the initial elevation.

249 Moreover, a new classification for the RMSE is proposed in this study, such that excellent represents a score lower than 0.25 m,
250 good between 0.25 m and 0.4 m, reasonable between 0.4 m and 0.6 m, poor between 0.6 m and 0.8 m and bad larger than 0.8 m. This
251 classification aims at complementing the van Rijn et al. (2003)'s classification. Furthermore, a coastal erosion indicator relevant for coastal
252 risks, and subsequently for EWSs, such as the dune toe retreat (Ferreira et al. 2017) was computed to further analyze differences in model
253 performance between the 1D and 2D schemes.

254 **RESULT**

255 **One-dimensional horizontal displacement sensitivity**

256 The 1D sensitivity analysis performed at the full-berm profile revealed that: 1) when the “wetslope” was set to 0.2 (upper panels
257 in Fig. 5), the horizontal retreat at 3 m was sensitive to “bermslope” and “facua”. The retreat decreased linearly with increasing values of
258 “facua” for all “bermslope” conditions. Moreover, when the “bermslope” was deactivated, higher erosion was computed (for the same
259 “facua”) than when it was activated. Furthermore, an increase of 0.02 in “bermslope” resulted in more than 20% less horizontal erosion. At
260 the berm height, “facua” was similarly important in controlling erosion. On the other hand, differences between “bermslope” off and 0.10
261 were minimum, but “bermslope” set to 0.12 reduced the retreat between 15 and 20%. At the dune toe, variations in “facua” still had an
262 almost linear relationship with horizontal erosion (except for “bermslope” 0.12), and the erosion can be reduced by 90% when setting
263 “facua” to 0.3 when compared to 0.15. The parameter “bermslope” was partially important; a value of 0.10 provided almost a similar
264 effect to deactivated, but 0.12 reduced the horizontal erosion, between 70 and 100% (null horizontal displacement). 2) When “bermslope”
265 was deactivated (middle panels Fig. 5), higher “wetslope” reduced retreat; an increase of 0.05 produced 5-10% approximately less erosion,
266 regardless of the value of “facua”. At the berm height, the influence of “wetslope” was higher, and increases of 0.05 decreased erosion by
267 12-18%. At the dune toe, “wetslope” played an essential role and with “facua” set to 0.15, “wetslope” of 0.25 and 0.3 can reduce the
268 erosion 70 and 100%, respectively, in respect to “wetslope” equal to 0.2. 3) when “bermslope” was set to 0.10 (lower panels in Fig. 5), the

269 model was not sensitive to changes on the “wetslope” at 3 m height. Moreover, the sensitivity to “wetslope” at the berm height was lower
270 than in the case when “bermslope” was deactivated. At the dune toe, the model was still sensitive to “wetslope”. Thus, with “facua” set to
271 0.15, “wetslope” of 0.25 and 0.3 can reduce the erosion by 40 and 70%, respectively, in comparison to “wetslope” equal to 0.2.

272 The weak-berm profile responded to changes at the tested parameters like the full-berm profile (Fig. 6), except at the dune toe,
273 where the model still maintained a certain sensitivity to the three parameters but was less sensitive than the full-berm profile. While all
274 runs performed on the weak-berm profile resulted in dune toe retreat, some runs performed on the full-berm profile did simulate no dune
275 retreat (Fig. 5 and Fig. 6).

276 **One-dimensional calibration and validation**

277 A total of 36 simulations were performed for each profile at Praia de Faro (see Table 3). The characteristics of the tested profiles
278 (Fig. 7) were reasonably different: F4 was shorter with a beach face slope of 0.12, and it was considered as non-erodible after the 3732 m
279 (cross-shore distance). F6 had a similar slope (0.11) but its backshore was wider and connected to a 6.5 m MSL height dune. For easier
280 visualization of the calibration exercise, both the van Rijn et al. (2003) and the RMSE classifications were transformed into a color code,
281 with excellent being represented by black and bad by white. The skills BSS and RMSE of the two analyzed profiles were averaged and
282 used to compare the performance of each simulation. The calibration results revealed that when “bermslope” was deactivated, “facua”
283 required the highest value assessed (0.3) to classify the model results as excellent (Table 4), regardless of the value of “wetslope”. As
284 “facua” was reduced, the performance of the model was reduced as well. When “bermslope” was set to 0.10, all simulations, in general,
285 resulted in high scores, especially simulations with “facua” equal to 0.20 and 0.25. Erosion was underestimated for simulations with
286 “facua” equal to 0.3 and overestimated when “facua” was set to 0.15 (not shown here). Finally, when “bermslope” was set to 0.12, it was
287 observed that decreasing “facua” improved the skills of the model; the best score was found with “facua” set to 0.15. Therefore, several
288 combinations of “facua”, “bermslope”, and “wetslope” yielded excellent for both skills, BSS and RMSE (see Table 4 where a cell entirely
289 black represents the best performance). Among these 36 simulations, the skills of the simulation with the highest scores for “bermslope”
290 off, 0.10, and 0.12 are presented in Table 5 - i, - ii, and - iii respectively. The simulations with “bermslope” activated obtained slightly
291 better skills than the simulations with “bermslope” off. The simulation with the lowest scores (“facua” = 0.15; “wetslope” = 0.4;
292 “bermslope” = off) is represented for comparison in Fig. 7 IV), highlighting the sensitivity of the model for the cases assessed in this
293 study.

294 **Two-dimensional simulations in Praia de Faro**

295 *Storm Emma*

296 The model results of the simulations shown in Table 5 - i, - ii, and - iii were plotted against the measurements taken after storm
297 Emma in Fig. 7 I – III (note that post-storm Emma measurements did not cover the dune in F6). The morphological changes simulated by
298 the 2D model using the same values for “facua”, “wetslope” and “bermslope” as the 1D model were represented as well (Fig. 7 I – III).
299 The comparison between the 1D and 2D model approaches showed that the modeled erosion at the beach face was, in general, slightly
300 higher
301 in the 1D approach, especially in F4 (Fig. 7 I – III). However, this comparison indicated that the erosion of the dune in F6 was
302 considerably larger in the 1D model than in the 2D model, with dune toe retreat differences up to 7 m in some runs (e.g. Table 5 - ii). In
303 general, the average BSS and RMSE (F4 and F6) for the 1D and 2D models were similar (Table 5). Among all setting combinations, and
304 after plotting several 2D results (not shown here), the best morphological representation of the storm-induced erosion was provided by the
305 simulation with “facua” = 0.15, “wetslope” = 0.2, and “bermslope” = 0.12, see Fig. 8. It does not exhibit entirely the best skills (Table 5 -
306 v), but these settings replicated more accurately the observed dune retreat (Garzon et al. 2021) while simulating also correctly the erosion
307 in the beach face. Furthermore, it is important to highlight two aspects: 1) when including “bermslope”, the erosion in all profiles was
308 reasonably well predicted (Fig. 8), including F3, whose initial profile showed a lower sand volume (beach cusp trough) compared for
309 instance with F2 (beach cusp crest). Conversely, when “bermslope” was deactivated the modeled erosion was overestimated (~ 1 m of
310 vertical erosion) in F3 (Fig. 8). Thus, including “bermslope” produced, in general, more consistent results along the five profiles; and 2)
311 the simulation with “bermslope” deactivated displayed a milder slope below 0 m MSL than the one with “bermslope” (Fig. 8). The value
312 of “bermslope” was similar to the actual beach face slopes found in the profiles F2-F6 that ranged between 0.09 and 0.12 (Fig. 8).

313 To further investigate discrepancies on the modeled erosion between the 1D and 2D approaches for storm Emma, the
314 hydrodynamic (wave height, sea level and infragravity wave height) and morphological outputs were plotted (Fig. 9). The two models, 1D
315 and 2D (using single direction) simulated similar wave height (Fig. 9 a) and sea level (Fig. 9 c), but the infragravity wave height computed
316 on the 1D model was higher than on the 2D model (Fig. 9 b). When comparing the final profile (Fig. 9 d), it can be concluded that dune
317 erosion was enhanced on the 1D model with regards to the 2D. Also, the outputs of the 1D model using both the single direction and
318 multiple direction options were contrasted in Fig. 9. The multiple direction approach computed slightly lower infragravity wave heights
319 than the single direction approach (but still higher than the 2D approach) as seen in Fig. 9 b, while the rest of the hydrodynamic variables
320 were similar (Fig. 9 a, c). When comparing the post-storm profiles in Fig. 9 d, it was observed that the three approaches simulated similar

321 erosion at the beach face (below 3 m above MSL) but large differences were found in the dune face. For instance, the dune retreat at 5 m
322 above MSL obtained on the 2D model, 1D approach - multiple directions and 1D approach - single direction was 0, 3 and 6 m
323 respectively, Fig. 9 d.

324 The spatial prediction of the seabed change for Praia de Faro is displayed in Fig. 10, where the red color represents erosion, blue
325 deposition and yellow minimal changes. Maximum vertical erosion of 2.5 m in the beach face was simulated but this erosion was not
326 uniform alongshore as the result of the alongshore variability induced by the presence of the beach cusps (Fig. 10). Also, Fig. 10
327 demonstrated the effect of the non-erodible layer to hinder the erosion in the urbanized area. Moreover, the transition between the erodible
328 and non-erodible regions was correctly simulated (Fig. 8 and Fig. 10).

329 *Storm Elsa*

330 A second storm, Elsa, with lower energy was used to validate the findings from storm Emma in Praia de Faro. The simulation
331 used the best setting determined in the previous section (Table 5 - v) for the 2D model. According to the van Rijn et al. (2003)
332 classification, the performance of the model can be stated as excellent for all profiles (Fig. 11), while the bias ranged between -0.16 m
333 (overpredicted erosion)
334 for F1, and -0.03 m for F2. Although storm Elsa and Emma had different energetic conditions (mid-energy and high-energy), the model
335 was able to successfully replicate the erosion driven by both events using the same model settings.

336 **Two-dimensional simulations in Quarteira**

337 *Storm Elsa*

338 The calibration was carried out on the Quarteira December grid and involved the same parameters presented before (Table 3).
339 The modeled profiles displayed a well-developed berm, especially on the eastern and central profiles of each pocket beach (Q1, Q2, Q4,
340 and Q5) and a beach face slope between 0.08 and 0.12 (Fig. 12). Model experiments (not shown here), revealed that conversely to Praia de
341 Faro, “bermslope” caused unrealistic overprediction of the erosion in the groin heads (updrift), and hence, this parameter was deactivated
342 for the rest of the simulations in this site. Thus, the best calibration established “facua” and “wetslope” set to 0.15 and 0.20 respectively,
343 and “bermslope” off. The BSS and RMSE scores for the eastern and central profiles of each pocket beach were classified as excellent,
344 based on the previously discussed classifications, as displayed in Table 6. It is important to point out that the model reduced its ability to
345 predict the morphology of the profiles immediately downdrift of the groins (Q3, Q6, Q9; see Fig. 12 and Table 6).

347 To evaluate the sensitivity of the model to the initial topography, storm Emma was simulated in the Quarteira site under the two
348 topography conditions, May and December of 2019. There were differences between the initial profiles in May and December (Fig. 13)
349 and for instance, the berm crest was notorious in the latter survey, while in May the transition from the berm to the beach face was
350 smoother, particularly in Q1, Q2, Q4 and Q5. Moreover, in the May survey, mainly in the eastern profiles of each pocket beach (Q1, Q4,
351 and Q7), the slope was milder and the volume of sediment above MSL was larger than in the December survey. The numerical settings
352 were equal to those used to calibrate storm Elsa. XBeach results for storm Emma showed that the outputs from the two considered grids,
353 May and December, were close (Fig. 13) and, for instance, the onshore limit of the eroded profile was similar for both initial conditions.
354 Even in profiles with clearly different morphologies such as Q1, Q4, and Q7, the final computed impact of the storm was almost
355 equivalent.

356 When simulating storm Elsa on the Quarteira May grid, XBeach was still able to fairly reproduce the erosion as well, even if the
357 profiles were different from the actual pre-storm morphology. However, the RMSE increased in almost all profiles suggesting a lower
358 performance. The largest differences in model performances were found in Q1, Q6, Q8, and Q9 (Table 6). In all profiles, the positive bias
359 increased for the May grid simulation with regards to the December grid, indicating that erosion underestimation was higher on the May
360 grid. The model ability to simulate erosion at profiles immediately downdrift of the groins (Q3, Q6, Q9) on the May grid was also low.

361 *Storm Emma*

362 Visual inspections after storm Emma revealed that erosion barely reached the urbanized area at Quarteira and that morphological
363 changes were more significant in the eastern side of each pocket beach (downdrift). It was hypothesized that the typically eastward
364 longshore transport before the storm might have accumulated more material updrift of the groins. Thus, as observed in Fig. 13, if there
365 was more available sediment, the erosion was higher in these regions tending to reach a similar equilibrium profile in the area. The
366 modeled results of storm Emma for Quarteira showed that the groins had a clear influence on the morphodynamic of this site, and the
367 erosion (volume and berm retreat) was more significant immediately updrift of the groins (Q1, Q4, and Q7), with a maximum vertical
368 erosion of 2.5 m (Fig. 14). The definition of these structures as non-erodible at the model settings allowed successfully replicating the
369 morphodynamic of this site. Thus, as it was also observed in the Praia de Faro simulations, the non-erodible layer implemented in the
370 model behaved properly (Fig. 14). The upper section of the eastern and central beaches was not eroded, while the erosion at the western
371 beach extended almost to the promenade (Fig. 14). It, in general, matched the field (visual) observations, confirming the positive
372 performance of the model.

373 DISCUSSION

374 One-dimensional model

375 As it has been previously highlighted (Bugajny et al. 2013; Elsayed and Oumeraci 2017; Simmons et al. 2019; Splinter and
376 Palmsten 2012; Vousdoukas et al. 2012b), the modeled horizontal erosion was sensitive to “facua”. In general, a linear relationship was
377 found between increasing this parameter and decreasing the percentage of horizontal erosion in this study (Fig. 5 and Fig. 6). Similarly,
378 van der Lugt et al. (2019) found that changes in erosion volume scaled linearly with “facua”. The model seemed more sensitive to changes
379 in “facua” in the dune toe for both considered profiles at Praia de Faro. One of the reasons was that the actual magnitude of the horizontal
380 retreat at the dune toe was lower than at 3 m or at the berm crest, and therefore small changes in the model results caused large differences
381 in terms of percentage. This also explained the bigger sensitivity found in the full-berm profile, since in this profile, the magnitude of the
382 horizontal retreat at the dune toe was smaller than at the weak-berm profile. For instance, variations in “facua” from 0.15 to 0.25
383 (“wetslope” = 0.2 and “bermslope” = off) can lead to changes at the dune toe retreat up to 2.2 m in both profiles. Thus, simulations with
384 “wetslope” equal to 0.25 caused 50% and 30% less retreat than the benchmark case for the full-berm and weak-berm profile respectively
385 (upper panels in Fig. 5 and Fig. 6). The model was also sensitive to “wetslope”, and increasing this parameter reduced the erosion,
386 particularly in the dune toe (mid and lower panels in Fig. 5 and Fig. 6), as was also observed by previous studies (Armaroli et al. 2013;
387 Cho et al. 2019; Vousdoukas et al. 2012b). This was especially observed when “bermslope” was off. When “bermslope” was set to 0.10,
388 the model was no longer sensitive to this parameter at 3 m height, and slightly sensitive at the berm height, but it was still sensitive at the
389 dune toe (lower panels in Fig. 5 and Fig. 6). This would partially agree with Roelvink et al. (2019) since they stated that “bermslope”
390 could replace the effect of “wetslope”. Also, an increase in “bermslope” produced an enhanced onshore sediment transport and the erosion
391 decreased with “bermslope” set to 0.12 (upper panels in Fig. 5 and Fig. 6) as Roelvink et al. (2019) found in their study.

392 The 1D calibration proved that several model combinations of “facua”, “wetslope”, and “bermslope” produced excellent results
393 for the evaluation of coastal erosion at steep beaches (Table 4). These results also confirmed that steep profiles required larger values of
394 “facua” than the default value to compensate for the onshore transport induced by the incident-band swash processes, which are not
395 included in XBeach (Elsayed and Oumeraci 2017; Roelvink and Costas 2017; Vousdoukas et al. 2012b). Moreover, it is important to
396 highlight that within the limits proposed on the RMSE-based and van Rijn et al. (2003) classifications, the sensitivity to “wetslope” was
397 low (Table 4). In the modeled profiles, the performance of XBeach was only evaluated up to 3 – 4 m MSL, and the dune erosion was not
398 considered (lack of measured data), where the avalanching and slumping processes controlled by “wetslope” are more significant. The
399 addition of the “bermslope” parameter and the reduction of “facua” resulted in an excellent model prediction in the tested steep profiles
400 with different berm morphologies. Thus, when “bermslope” was set to 0.10 and 0.12, “facua” values of 0.2 and 0.15 produced excellent

401 results. Roelvink et al. (2019) also noticed that the combination of a moderate “bermslope” and low “facua” provided good results.
402 Similary, Lashley et al. (2019) found that only when “bermslope” was activated, the model was able to reproduce the steep post-storm
403 dune profile.

404 **Two-dimensional model**

405 The same parameters were used to calibrate the 2D model in Praia de Faro yielding several combinations of excellent results. As
406 it was found in the 1D calibration, when “bermslope” was off and “facua” was set to 0.3, the model tended to provide accurate results
407 (Table 5). However, when “bermslope” was included, excellent results were obtained for several combinations. This confirmed that the
408 inclusion and use of “bermslope” were also adequate for a two-dimensional XBeach model for steep beaches. Moreover, the use of
409 “bermslope” reduced the variability between profiles, providing more robust results alongshore (Fig. 8). The post-storm profiles presented
410 a relatively uniform behavior despite the existence of a pre-storm alongshore variability due to the presence of beach cusps (Vousdoulas et
411 al. 2012a). It is important to note that the model parametrization providing the most accurate results used values that were close to the
412 values recommended in the XBeach manual for “facua” and “wetslope”. This can avoid the model behaving abnormally (e.g. excessive
413 profile flattening around the waterline) as a consequence of unusual values on those model parameters, as observed in Fig. 8 and
414 previously reported by other authors such as Simmons et al. (2019). Furthermore, the value of “bermslope” chosen here was similar to the
415 beach face slope found in the study area (Fig. 8 and Fig. 11). As the present work only focused on destructive processes induced by
416 storms, these settings might not be appropriate to simulate constructive morphological processes in the long term as found by Kombiadou
417 et al. (2021).

418 The comparison between the 1D and 2D hydrodynamic and morphological outputs for the high-energy storm Emma
419 demonstrated that the higher erosion simulated by the 1D model was related to the higher infragravity wave height simulated on the one-
420 dimensional model (Fig. 9). Different model domains (1D or 2D) and different wave spreading approaches (“single_dir” and “multi_dir”)
421 resulted in discrepancies in the simulated infragravity energy, Fig. 9 b. Roelvink and Reniers (2012) declared that the swash processes in
422 the infragravity band play an essential role in the avalanching mechanism, one of the main factors in dune erosion. Thus, the authors
423 hypothesized that the larger energy of the infragravity band of the 1D model might lead to an enhanced erosion of the dune in respect to
424 the 2D model, as observed in Fig. 7 and Fig. 9 d. Roelvink et al. (2018) also stated that the 1D model with “single_dir” simulated higher
425 runup in steep beaches than a 2D model using “single_dir” as well, confirming the results depicted in Fig. 9. In fact, they compared model
426 results against field observations and noted that the 2D model was able to predict the runup while the 1D overestimated the measurements.

427 On the other hand, the beach face seemed similarly eroded at the end of the storm with both the 1D and 2D approaches (Fig. 7 and Fig. 9
428 d.)

429 The good performance of the model in Praia de Faro to simulate the erosion caused by the mid-energy storm Elsa demonstrated
430 that the results obtained in a calibration process, for one storm, can be applied to successfully validate a second storm, even with different
431 severity. This statement agrees with Simmons et al. (2019) that found that a second storm modestly improved the calibration results and
432 suggested that coastal practitioners should focus more on collecting data in more locations rather than collecting data for several storms.
433 Nevertheless, the findings of this site cannot be transferred to another site located just 10 km away (Quarteira). XBeach applied to
434 Quarteira was also successfully validated, quantitatively and qualitatively, for storms Emma and Elsa, but the parametrization providing
435 good results in Praia de Faro failed in predicting the erosion in Quarteira. Conversely to the Praia de Faro model, “bermslope” did not
436 provide satisfactory results in Quarteira. The model faced large problems to simulate morphological changes around the groins, and highly
437 overestimated the erosion. When “bermslope” was off, it can be observed that the value of “facua” in this site was considerably lower than
438 in the Praia de Faro model. It is not totally understood why the model required lower onshore transport since the profiles also presented a
439 steep beach face slope. Some of the reasons can be associated with the presence of the groins. Bugajny et al. (2013) carried out several 1D
440 XBeach model simulations in unprotected, protected, and heavily protected coasts and they noticed a decrease in “facua” with an increase
441 of the engineering protection, reporting values of “facua” of 0.5, 0.3 and 0.1, respectively. Further investigations of the role of “facua” in
442 protected coasts are suggested to shed some light on this process. Moreover, the good skills of the model simulating erosion under the
443 impact of two very different storms (high-energy and mid-energy) demonstrated these calibration parameters produce adequate results for
444 both hydrodynamic conditions.

445 Elevation measurements immediately before the storm in the surf zone area and the dry beach are not always available and
446 model experiments might have to use data only collected weeks or months prior to the storm. This gap in time might lead to some errors
447 or uncertainties when evaluating morphodynamic models. The comparison between the outputs from the Quarteira May and December
448 grids proved that the model was largely more sensitive to input parameters than initial topography, mainly if the initial different
449 morphologies still represented similar beach volumes, which is in line with other studies, such as Armaroli et al. (2013). This was
450 especially evident for the high-energy storm (Emma) when compared to the mid-energy storm (Elsa).

451 **Recommendations for XBeach implementation on steep beaches**

452 When implementing the XBeach model in an unexplored steep beach, the first efforts should be focused on collecting field data
453 to validate and calibrate the morphodynamic model. This has special relevance in reflective beaches since all wave processes occurring in
454 the swash zone of these types of environments are not totally reproduced by models, namely XBeach (surfbeat). Thus, a default model

455 parametrization could provide completely erroneous results. In the case of the lack of data for model validation and calibration, modelers
456 working on exposed steep profiles should pay attention to “facua” and “bermslope”. In these beaches, values of “facua” close to the default
457 value only perform properly when “bermslope” is activated and acceptable results can be obtained by using several combinations of these
458 two parameters. A tentative value for “bermslope” can be the beach face slope of the profiles. Moreover, if a dune system is present, the
459 “wetslope” value must be carefully chosen but it might be close to the recommended value in the XBeach manual. On the other hand, if
460 the reflective site presents engineering protection structures such as groins, the impact of the wave asymmetry sediment transport is lower
461 and consequently, values of “facua” must be reduced. The use of the “bermslope” in these protected sites must be carefully assessed as
462 might largely overestimate the erosion. Furthermore, the model would not require to be calibrated against several storms, for both
463 landscapes (exposed and groin-protected sites), which is an advantage for designing and predictive purposes.

464 While the 1D and 2D models simulate similar erosion in the beach face (using the same model parametrization), the erosion
465 predicted at the upper beach and in the dune by a 1D cross-shore model was higher than the erosion computed on a two-dimensional grid.
466 Therefore, if the dune erosion is a major concern, different model parametrization is required in a one and two-dimensional model. This is
467 especially important for the design of coastal interventions, namely if dealing with risk. Thus, at an initial phase, both approaches should
468 be tested against observations to find the optimum parametrization for the 1D and 2D models. If the computational power is a major
469 limitation, then multiple 1D simulations are preferable to a 2D model. Moreover, “single_dir” is more efficient than the “multi_dir”
470 approach (Roelvink et al. 2018).

471 A systematic collection of elevation data can be very challenging. Thus, numerical models usually rely on a static initial topo-
472 bathymetry, i.e., the elevation of the grid is not updated. In highly dynamic environments such as sandy beaches, this might result in some
473 limitations, adding some uncertainties to the predicted morphological changes. However, even for different pre-storm profile
474 morphologies, if they maintain approximately the same amount of sand volume, the predicted erosion (post-storm shoreline and berm
475 position) on those different morphologies is similar, mostly for high energetic storms. This would imply that the topography of the model
476 does not need to be periodically updated, particularly when taking into consideration the impact of storms with high energy or return
477 period. Furthermore, steep beaches exhibit a rapid post-storm recovery response and they are able to gain a large part of the eroded
478 material in the order of weeks, supporting the idea that the static initial elevation approach would be sufficient to obtain reliable model
479 results.

480 **CONCLUSIONS**

481 Complex morphodynamic models are suitable to assess and investigate the storm impact in coastal areas. However, these models
482 can be sensitive to a large number of free parameters and require calibration and validation. The sensitivity and performance of XBeach

483 have been mainly investigated in mild slope beaches where the saturated surf zone condition is matched, while model behavior in steep
484 beaches has received less attention. Here, numerical experiments were combined with topographical measurements collected for two large
485 storms (16-yr and 5-yr return period) to obtain reliable settings for better model performance in steep beaches. These experiments
486 demonstrated that: 1) the model was sensitive to “facua” (parameterized wave asymmetry sediment transport component), “bermslope”
487 (upslope swash zone transport term), and “wetslope” (critical avalanching slope) when simulating high energy storms. However, if
488 “bermslope” was activated, the effect of “wetslope” was reduced in the beach face but still relevant in the dune face; 2) the model
489 calibration in an exposed beach (Praia de Faro) for a high-energy storm showed that when “bermslope” increased, “facua” must be
490 reduced, and vice versa, to properly simulate the erosion. Moreover, “bermslope” reduced the model results variability alongshore,
491 minimizing the effect of upper beach face cusps on the final model erosion; 3) with similar settings, 1D and 2D models simulated similar
492 erosion in the beach face, but the erosion in the dune increased in the 1D simulations; 4) after calibrating with one storm, the 2D model
493 ability to simulate erosion during two storms was classified as excellent. The value of “bermslope” can be related to the beach face slope
494 and it contributed to the utilization of values of “facua” and “wetslope” close to the default values; 5) in a groin-protected site, Quarteira,
495 the 2D model was also successfully validated, although required different settings when compared to the exposed beach. Also, the
496 predicted erosion in this site was not especially sensitive to initial beach topography. These findings demonstrate that these parameters
497 produce adequate results for both hydrodynamic conditions and coastal settings. This work provides new insights on how to improve the
498 modeling of coastal erosion processes in steep beaches and supports the implementation of morphodynamic models at exposed and groin-
499 protected beaches.

500 **Data Availability Statement**

501 All data, models, or codes that support the findings of this study are available from the corresponding author upon reasonable request.

502 **Acknowledgments**

503 This work is supported by the EW-COAST project with reference ALG-LISBOA-01-145-FEDER-028657 and attributed by the
504 Portuguese Foundation of Science and Technology (FCT), supported by the Regional Operational Program of Algarve and the Regional
505 Operational Program of Lisbon in its component FEDER and the Foundation for Science and Technology in its OE component. The
506 authors would like to acknowledge the financial support of FCT to CIMA through UIDP/00350/2020. We also acknowledge Professor
507 Joaquim Luis for sharing bathymetric information (<http://w3.uaalg.pt/~jluis/mirone/main.html>) and Luísa Bon de Sousa for data acquisition
508 and processing. Also, the Instituto Hidrográfico and Puertos del Estado are acknowledged for supplying wave and water level data, and

509 Sebastião Teixeira (APA) for providing the bathymetric data. COSMO Program under *Programa de Monitorização da Faixa Costeira de*
510 *Portugal Continental* (COSMO), of APA, co-funded by the *Programa Operacional Sustentabilidade e Eficiência no Uso de Recursos*
511 (POSEUR) is acknowledged. Dr Plomaritis was funded by the 2014-2020 ERDF Operational Programme and by the Department of
512 Economy, Knowledge, Business and University of the Regional Government of Andalusia with reference FEDER-UCA18-107062 and
513 Spanish Ministry of Science and Innovation, project code PID2019-109143RB-I00.

514 **References**

- 515 Almeida, L. P., Voudoukas, M. V., Ferreira, Ó., Rodrigues, B. A., and Matias, A. (2012). “Thresholds for storm impacts on an exposed sandy coastal area
516 in southern Portugal.” *Geomorphology*, Elsevier B.V., 143–144, 3–12.
- 517 Armaroli, C., Grotoli, E., Harley, M. D., and Ciavola, P. (2013). “Beach morphodynamics and types of foredune erosion generated by storms along the
518 Emilia-Romagna coastline, Italy.” *Geomorphology*, 199, 22–35.
- 519 Booij, N., Ris, R. C., and Holthuijsen, L. H. (1999). “A third-generation wave model for coastal regions: 1. Model description and validation.” *Journal of*
520 *Geophysical Research: Oceans*, 104(C4), 7649–7666.
- 521 Bugajny, N., Furmańczyk, K., Dudzińska-Nowak, J., and Papińska-Swerpel, B. (2013). “Modelling morphological changes of beach and dune induced by
522 storm on the Southern Baltic coast using XBeach (case study: Dziwnow Spit).” *Journal of Coastal Research*, Coastal Education and Research
523 Foundation, 65, 672–677.
- 524 Callaghan, D. P., Ranasinghe, R., and Roelvink, D. (2013). “Probabilistic estimation of storm erosion using analytical, semi-empirical, and process based
525 storm erosion models.” *Coastal Engineering*, Elsevier B.V., 82, 64–75.
- 526 Cho, M., Yoon, H.-D., Yang, J.-A., and Son, S. (2019). “Sensitivity and uncertainty analysis of coastal numerical model under various beach conditions in
527 Korea.” *Proceedings of the 9th International Conference, Coastal Sediment 2019*, 481–487.
- 528 Dissanayake, P., Brown, J., and Karunarathna, H. (2014). “Modelling storm-induced beach/dune evolution: Sefton coast, Liverpool Bay, UK.” *Marine*
529 *Geology*, Elsevier B.V., 357, 225–242.
- 530 Do, K., Shin, S., Cox, D., and Yoo, J. (2018). “Numerical Simulation and Large-Scale Physical Modelling of Coastal Sand Dune Erosion.” *Journal of*
531 *Coastal Research*, 85, 196–200.
- 532 Documentation XBeach. (2018). “Release XBeach v1.23.5527 XBeachX FINAL. November.”
- 533 Elsayed, S. M., and Oumeraci, H. (2017). “Effect of beach slope and grain-stabilization on coastal sediment transport: An attempt to overcome the erosion
534 overestimation by XBeach.” *Coastal Engineering*, Elsevier, 121(June 2016), 179–196.
- 535 Ferreira, Ó., Matias, A., and Pacheco, A. (2016). “The East Coast of Algarve: a Barrier Island Dominated Coast.” *Thalassas: An International Journal of*
536 *Marine Sciences*, 32(2), 75–85.
- 537 Ferreira, Ó., Plomaritis, T. A., and Costas, S. (2017). “Process-based indicators to assess storm induced coastal hazards.” *Earth-Science Reviews*, Elsevier,
538 173(August), 159–167.
- 539 Ferreira, Ó., Plomaritis, T. A., and Costas, S. (2019). “Effectiveness assessment of risk reduction measures at coastal areas using a decision support system:
540 Findings from Emma storm.” *Science of the Total Environment*, 657, 124–135.
- 541 Garzon, J., Ferreira, A., Ferreira, Ó., Fortes, C., and Reis, M. (2020). *Beach State Report: Quarteira, Praia de Faro and Costa da Caparica*.
- 542 Garzon, J. L., Costas, S., and Ferreira, O. (2021). “Biotic and abiotic factors governing dune response to storm events.” *Earth Surface Processes and*
543 *Landforms*, (November), 1–19.
- 544 Gharagozlou, A., Dietrich, J. C., Karanci, A., Luettich, R. A., and Overton, M. F. (2020). “Storm-driven erosion and inundation of barrier islands from
545 dune-to region-scales.” *Coastal Engineering*, Elsevier B.V., 158.
- 546 Harter, C., and Figlus, J. (2017). “Numerical modeling of the morphodynamic response of a low-lying barrier island beach and foredune system inundated

547 during Hurricane Ike using XBeach and CSHORE.” *Coastal Engineering*, Elsevier, 120(November 2016), 64–74.

548 Kombiadou, K., Costas, S., and Roelvink, D. (2021). “Simulating destructive and constructive morphodynamic processes in steep beaches.” *Journal of*
549 *Marine Science and Engineering*, 9(1), 1–19.

550 Lashley, C. H., Bertin, X., Roelvink, D., and Arnaud, G. (2019). “Contribution of infragravity waves to run-up and overwash in the pertuis breton
551 embayment (France).” *Journal of Marine Science and Engineering*, 7(7).

552 van der Lugt, M. A., Quataert, E., van Dongeren, A., van Ormondt, M., and Sherwood, C. R. (2019). “Morphodynamic modeling of the response of two
553 barrier islands to Atlantic hurricane forcing.” *Estuarine, Coastal and Shelf Science*, Elsevier Ltd, 229(May), 106404.

554 Matias, A., Ferreira, Ó., Vila-Concejo, A., Morris, B., and Dias, J. A. (2010). “Short-term morphodynamics of non-storm overwash.” *Marine Geology*,
555 274(1–4), 69–84.

556 McCall, R. T., de Vries, J. S. M. V. T., Plant, N. G., Dongeren, A. R. Van, Roelvink, J. A., Thompson, D. M., and Reniers, A. J. H. M. (2010). “Two-
557 dimensional time dependent hurricane overwash and erosion modeling at Santa Rosa Island.” *Coastal Engineering*, 57(7), 668–683.

558 Orzech, M. D., Reniers, A. J. H. M., Thornton, E. B., and MacMahan, J. H. (2011). “Megacusps on rip channel bathymetry: Observations and modeling.”
559 *Coastal Engineering*, Elsevier B.V., 58(9), 890–907.

560 Pinto, C., Silveira, T. ., and Teixeira, S. B. (2018). “Alimentação artificial de praias na faixa costeira de Portugal Continental: Enquadramento e retrospectiva
561 das intervenções realizadas (1950- 2017).” *Relatório Técnico. Agência Portuguesa do Ambiente*. 60p.

562 Pires, H. O. (1998). “Project INDIA. Preliminary report on wave climate at Faro. Instituto de Meteorologia, IST, Lisboa, Portugal.”

563 Plomaritis, T. A., Costas, S., and Ferreira, O. (2018). “Use of a Bayesian Network for coastal hazards, impact and disaster risk.” *Coastal Engineering*,
564 134(February 2017), 134–147.

565 PROGRAMA COSMO. (n.d.). “<https://cosmo.apambiente.pt>, accessed in 02/11/2018.”

566 van Rijn, L. C., Wasltra, D. J. R., Grasmeyer, B., Sutherland, J., Pan, S., and Sierra, J. P. (2003). “The predictability of cross-shore bed evolution of sandy
567 beaches at the time scale of storms and seasons using process-based profile models.” *Coastal Engineering*, 47(3), 295–327.

568 Roelvink, D., and Costas, S. (2017). “Beach berms as an essential link between subaqueous and subaerial beach/dune profiles.” *Geotemas* 17, 79–82.

569 Roelvink, D., McCall, R., Costas, S., and van der Lugt, M. A. (2019). “Controlling swash zone slope is key to beach profile modelling.” *Proceedings of the*
570 *9th International Conference, Coastal Sediment 2019*, 149,157.

571 Roelvink, D., McCall, R., Mehvar, S., Nederhoff, K., and Dastgheib, A. (2018). “Improving predictions of swash dynamics in XBeach: The role of
572 groupiness and incident-band runup.” *Coastal Engineering*, The Authors, 134(February 2017), 103–123.

573 Roelvink, D., and Reniers, A. (2012). *A guide to modeling coastal morphology. Advances in Coastal and Ocean Engineering*, Singapore.

574 Roelvink, D., Reniers, A., van Dongeren, A., van Thiel de Vries, J., McCall, R., and Lescinski, J. (2009). “Modelling storm impacts on beaches, dunes and
575 barrier islands.” *Coastal Engineering*, 56(11–12), 1133–1152.

576 Simmons, J. A., Splinter, K. D., Harley, M. D., and Turner, I. L. (2019). “Calibration data requirements for modelling subaerial beach storm erosion.”
577 *Coastal Engineering*, Elsevier, 152(November 2018), 103507.

578 Smallegan, S. M., Irish, J. L., Van Dongeren, A. R., and Den Bieman, J. P. (2016). “Morphological response of a sandy barrier island with a buried seawall
579 during Hurricane Sandy.” *Coastal Engineering*, Elsevier B.V., 110, 102–110.

580 Splinter, K. D., and Palmsten, M. L. (2012). “Modeling dune response to an East Coast Low.” *Marine Geology*, Elsevier B.V., 329–331, 46–57.

581 Van Thiel de Vries. (2009). “Beach and dune erosion during storm surges.” Delft University of Technology.

582 Vousdoukas, M. I., Almeida, L. P. M., and Ferreira, Ó. (2012a). “Beach erosion and recovery during consecutive storms at a steep-sloping, meso-tidal
583 beach.” *Earth Surface Processes and Landforms*, 37(6), 583–593.

584 Vousdoukas, M. I., Ferreira, Ó., Almeida, L. P., and Pacheco, A. (2012b). “Toward reliable storm-hazard forecasts: XBeach calibration and its potential
585 application in an operational early-warning system.” *Ocean Dynamics*, 62(7), 1001–1015.

586

587

TABLE 1. Topo-bathymetric dataset sources and date of acquisition. All sources were referred to MSL

Praia de Faro		
Data acquisition methodology	Survey date	Profiles
Walking DGPS topographic profiles	March 2, 2018	F2, F3, F4, F5, F6
Unmanned aerial vehicle (COSMO program)	October 2018	All
Bathymetry survey (COSMO program)	October 2018	Not applicable
Walking DGPS topographic profiles	December 20, 2019	F1, F2, F3, F5
Quarteira		
Data acquisition methodology	Survey date	Profiles
APA bathymetric survey	2018	Not applicable
Unmanned aerial vehicle	May 28, 2019	All
Walking DGPS topographic profiles	December 17, 2019	Q1-Q9
Walking DGPS topographic profiles	December 20, 2019	Q1-Q9

588

589

TABLE 2. Main numerical parameters and their values

Parameter	Value
break	Roelvink2
gamma	0.56
alpha	1.0
turb	wave_averaged
Single_dir	On
Lateral wave type	Cyclic
Lateral flow condition	Neumann
Morfac	10
Factor bed slope effect	0.15
dzmax	0.05
h _{switch}	0.01
dryslope	1

590

591

TABLE 3. Parameters evaluated in the sensitivity analysis and the calibration exercise

Parameter	Default	XBeach manual range	Values tested
Facua	0.1	0.0 – 1.0	0.15, 0.20, 0.25, 0.30
Wetslope	0.3	0.2 – 1.0	0.20, 0.25, 0.30, 0.40*
Berm slope	off	0.0 – 1.0	Off, 0.10, 0.12

592

* 0.4 was not evaluated in the sensitivity analysis.

593

594

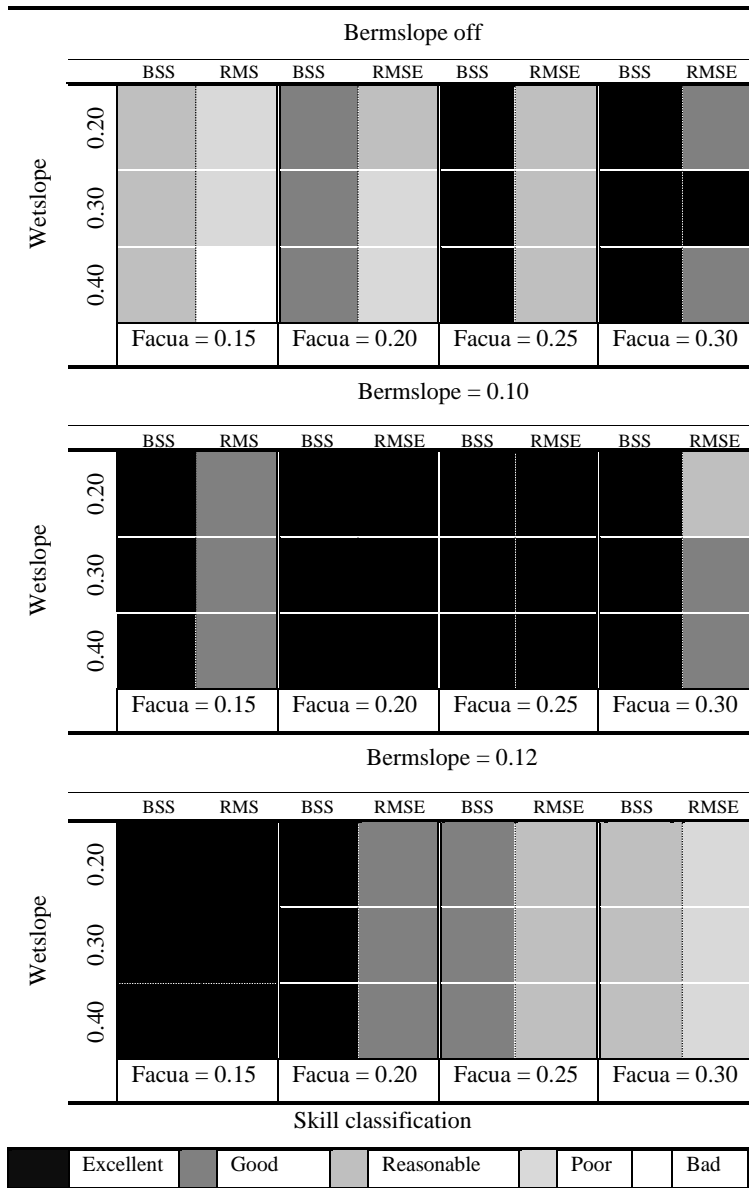
595

596

597

598

TABLE 4. Model skill classification, based on the average of the two skills BSS and RMSE. Left boxes, inside each table cell, represent the colour code for the BSS classification and right boxes indicate the RMSE classification.



599

600

601

602 **TABLE 5.** One-dimensional and two-dimensional skill comparison calculated by averaging F4 and F6, and all profiles after storm Emma.

#	Parameters			Average BSS			Average RMSE			Dune toe retreat (m) at F6	
	Bermslope	Facua	Wetslope	1D	2D*	2D**	1D	2D*	2D**	1D	2D
i	Off	0.30	0.30	0.95	0.96	0.86	0.24	0.21	0.31	4.3	0
ii	0.10	0.20	0.40	0.97	0.97	0.95	0.20	0.18	0.23	7.3	0.4
iii	0.12	0.15	0.40	0.97	0.97	0.95	0.20	0.21	0.24	5.3	0.3
iv	0.10	0.20	0.20	0.95	0.94	0.94	0.24	0.26	0.28	12.0	3.3
v	0.12	0.15	0.20	0.94	0.94	0.95	0.24	0.26	0.26	9.3	2.7

603 2D*: averaging F4 and F6; 2D**: averaging all profiles.

604 **TABLE 6.** Statistical skills for the Quarteira December and Quarteira May grids for storm Elsa.

December grid	Q1	Q2	Q3	Q4	Q5	Q6	Q7	Q8	Q9
BSS	0.95	0.90	0.61	0.96	0.90	0.80	/	0.83	0.49
RMSE, m	0.17	0.19	0.31	0.15	0.18	0.20	/	0.22	0.43
Bias, m	0.03	0.09	0.15	-0.13	0.03	0.10	/	0.09	0.35
May grid	Q1	Q2	Q3	Q4	Q5	Q6	Q7	Q8	Q9
BSS	0.90	0.91	0.69	0.97	0.95	0.65	0.93	0.76	0.34
RMSE, m	0.40	0.22	0.41	0.21	0.17	0.38	0.19	0.46	0.61
Bias, m	0.36	0.17	0.37	0.19	0	0.32	0.08	0.37	0.58

605
606

607 **Fig. 1.** I) The Iberian Peninsula with the marker indicating the study area. II) Study area location within the Portuguese southern coast. The
608 black square displays the location of both the Faro buoy and the Puertos del Estado forecast output. III) Location of the Quarteira and
609 Praia de Faro grid models and the bathymetric lines. IV) Praia de Faro study area. V) Three beach segments in the Quarteira study area
610 limited by the perpendicular groins. The black lines indicate the cross-shore profiles analyzed. The background image sources are Esri,
611 HERE, Garmin, OpenStreetMap contributors, and the GIS user community.

612 **Fig. 2.** Left plots display the hydrodynamic conditions during storm Emma 2018. The wave characteristics were measured at the Faro buoy
613 (<https://www.hidrografico.pt/boias>) and the water levels were extracted from the tidal gage of Huelva (Spain). The right plots represent the
614 wave conditions provided by the wave prediction system of Puertos del Estado ([http://www.puertos.es/en-](http://www.puertos.es/en-us/oceanografia/Pages/portus.aspx)
615 [us/oceanografia/Pages/portus.aspx](http://www.puertos.es/en-us/oceanografia/Pages/portus.aspx)) during storm Daniel and Elsa 2019 (Faro buoy was not recording) and the water level measured at
616 Huelva. The blue box at the right plots indicates the duration of the storm considered in the XBeach simulations. For storm Emma, the
617 model was initiated on February 28, 2018, 00:00, and finished on March 2, 2018, 18:00. For storm Elsa, the model started on December
618 18, 2019, 00:00 and finished on December 20, 2019, 18:00.

619 **Fig. 3.** One-dimensional profiles evaluated in the sensitivity analysis: a) full berm profile and b) weak berm profile. The squares represent
620 the displacement analysis location with the upper one representing the dune toe at both profiles, the intermediate one the berm crest and
621 the lower one the 3 m MSL elevation (landward beach face).

622 **Fig. 4.** Modeling exercises at Praia de Faro (upper-half) and Quarteira (lower-half) displaying the analyzed model scheme (one or two-
623 dimensional), the goal of the exercise, the simulated event and the topographical dataset interpolated in the model grid. The horizontal
624 arrows show the interactions between the runs.

625 **Fig. 5.** Full-berm profile sensitivity results displayed as erosion percentage against the value of “facua”. In the upper plots, the “wetslope”
626 is equal to 0.20. In the middle plots, “bermslope” was deactivated and in the lower plots, the “bermslope” was 0.10.

627 **Fig. 6.** Weak-berm profile sensitivity results displayed as erosion percentage against the value of “facua”. In the upper plots, the
628 “wetslope” is equal to 0.20. In the middle plots, “bermslope” was deactivated and in the lower plots, the “bermslope” was 0.10.

629 **Fig. 7.** Model results produced by the parametrization displayed on: I) Table 5 - i, II) Table 5 - ii, III) Table 5 - iii, and IV) The simulation
630 with the lowest score. Left plots display the F4 profile and right panels F6 profile.

631 **Fig. 8.** Five cross-shore profiles extracted from the two-dimensional model. The simulations correspond to Table 5 - i and Table 5 - v for
632 storm Emma.

633 **Fig. 9.** (a) Sea level plus the root mean square of the wave height (H_{rms}) and the modeled beach profile on the peak of storm Emma, (b)
634 Root mean square of the infragravity wave height (H_{rmsIG}) plus the sea level and the modeled beach profile on the peak of the storm, (c)
635 sea level and the modeled beach profile on the peak of the storm, (d) Simulated post-storm profiles. In the four subplots, the solid lines
636 illustrate the 2D model, the crossed dot lines the 1D model with a single direction, and the dashed line the 1D model with multi-direction.

637 **Fig. 10.** A) Bottom elevation difference (post minus pre-storm) induced by storm Emma in Praia de Faro at the parking lot area (F4 and
638 F5), left side and location of the F2, right side. The background image source is Esri, extracted from the GIS User Community.

639 **Fig. 11.** Measurements against model results in four profiles of Praia de Faro for storm Elsa.

640 **Fig. 12.** Measurements against model results in eight profiles of the Quarteira December grid for storm Elsa. The value of “facua” and
641 “wetslope” were 0.15 and 0.20 respectively, and the “bermslope” was deactivated.

642 **Fig. 13.** Model results predicted by the 2D models of Quarteira during storm Emma.

643 **Fig. 14.** Bottom elevation difference (post minus pre-storm) induced by storm Emma in Quarteira, using the input elevation from the
644 survey of May 2019. The value of “facua” and “wetslope” were 0.15 and 0.20 respectively, and the “bermslope” was deactivated. The
645 background image source is Esri, extracted from the GIS User Community.

646

647